Supplemental Materials

The energy spectrum of major waves in the DYNAMO IOP observation and in our CTRL simulation and experiments is obtained from using the same method described in Wang et al. (2015). This method is a regional version of the global Wheeler and Kiladis diagram (Wheeler and Kiladis 1999). In this regional analysis, the background spectrum (defined as smoothed spectrum) is removed, and the symmetric components are obtained using the DYNAMO IOP data and the date of our CTRL simulation and experiments. They are shown in Fig. S1. Note that in Fig. S1, westward propagating equatorial Rossby waves ($n = 1$) are not shown because of their insignificant energy amount compared to the other waves shown in Fig. S1.

The CTRL result in Fig. S1b has a very similar energy spectrum of waves as the observed in Fig. S1a, both showing large amount of energy concentrated in quasi-stationary oscillations and eastward propagating waves of intraseasonal frequency. Moreover, the power of the eastward propagating waves in Figs. S1a and S1b is along a line far to the right of the Kelvin wave ($n = -1$) with the equivalent depth of 12 m. This difference indicates that those eastward propagating waves of large energy are much slower than the Kelvin wave of the equivalent depth of 12 m. If an additional Kelvin wave of an equivalent depth smaller than 12 m were added in Figs. S1a or S1b to match the energy distribution for those eastward propagating waves the phase speed of that wave would have been slower at a phase speed comparable to those waves migrating eastward. However, the smaller equivalent depth would be indicating a higher internal mode which would have a much shallower heating profile utterly different from the observed and the CTRL (Figs. 6 and 7). It is therefore reasonable to believe that those eastward propagating waves of intraseasonal frequency are highly likely forced by the variations of deep convection arising from the cloud radiative effect and feedbacks (including the large-scale horizontal and vertical convergence of mass, moisture, and energy as shown in Figs. 7 and 9).

This notion is also supported by the difference between these observed and CTRL result and the result in Fig. S1c from EXP1. Figure S1c shows very small amount of energy in the quasi-stationary oscillation and eastward propagating waves. Those eastward waves are more aligned with the Kelvin wave of 12 m equivalent depth and have fast phase speed. They suggest that in the absence of deep convection regular/intrinsic eastward propagating Kelvin waves along with the westward travelling inertial-gravity waves are dominant, as anticipated for convection-free atmosphere. Weak quasi-stationary intraseasonal frequency variations also exist in this

environment as suggested by the energy spectrum in Fig. S1c. As discussed in the main text, they could be the embryos waiting for proper conditions to grow and develop into MJO events.

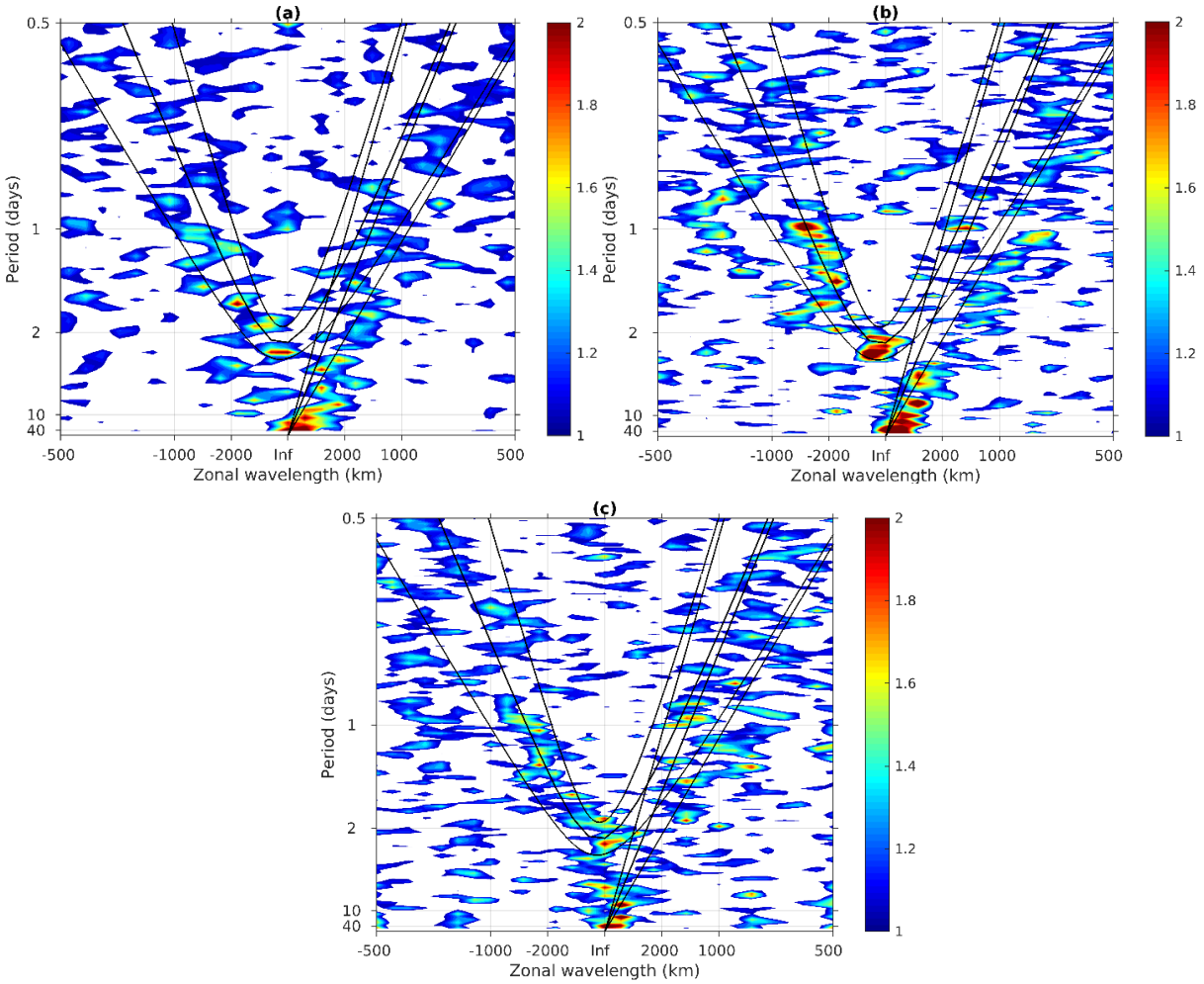

Figure S1: Power of waves in the wavelength–frequency diagram (Wheeler and Kiladis 1999) derived from 3-hourly surface precipitation in the model domain (50°-120°E) averaged between 5°S and 5°N; (a) observed, (b) CTRL, and (c) EXP1. The three V-shaped curves correspond to $n = 1$ inertia–gravity waves with equivalent depths of 12, 25, and 50 m (from bottom to top). The three straight lines are for $n = -1$ Kelvin waves with equivalent depths of 12, 25, and 50 m (from right to left).